Published in final edited form as:

Microb Pathog. 2014 August ; 73: 70–79. doi:10.1016/j.micpath.2014.04.005.

Follistatin-like protein 1 is a critical mediator of experimental Lyme arthritis and the humoral response to *Borrelia burgdorferi* infection

Brian T. Campfield[a], **Christi L. Nolder**[a], **Anthony Marinov**[a], **Daniel Bushnell**[a], **Amy Davis**[b], **Caressa Spychala**[a], **Raphael Hirsch**[a], and **Andrew J. Nowalk**[a]

Andrew J. Nowalk: nowaaj@chp.edu, andrew.nowalk@chp.edu

[a]Department of Pediatrics, University of Pittsburgh School of Medicine, 4401 Penn Avenue, Pittsburgh, PA 15224, USA

[b]Department of Pathology, University of Pittsburgh School of Medicine, 4401 Penn Avenue, Pittsburgh, PA 15224, USA

Abstract

Follistatin-like protein 1 (FSTL-1) has recently been described as a critical mediator of CIA and a marker of disease activity. Lyme arthritis, caused by *Borrelia burgdorferi*, shares similarities with autoimmune arthritis and the experimental murine model collagen-induced arthritis (CIA). Because FSTL-1 is important in CIA and autoimmune arthritides, and Lyme arthritis shares similarities with CIA, we hypothesized that FSTL-1 may be an important mediator of Lyme arthritis. We demonstrate for the first time that FSTL-1 is induced by *B. burgdorferi* infection and is required for the development of Lyme arthritis in a murine model, utilizing a gene insertion to generate FSTL-1 hypomorphic mice. Using qPCR and qRT-PCR, we found that despite similar early infectious burden, FSTL-1 hypomorphic mice have improved spirochetal clearance in the face of attenuated arthritis and inflammatory cytokine production. Further, FSTL-1 mediates pathogen-specific antibody production and antigen recognition when assessed by ELISA and one- and two-dimensional immunoblotting. This study is the first to describe a role for FSTL-1 in the development of Lyme arthritis and anti-*Borrelia* response, and the first to demonstrate a role for FSTL-1 in response to infection, highlighting the potential for FSTL-1 as a target in the treatment of *B. burgdorferi* infection.

Keywords

Borrelia burgdorferi; Lyme disease; FSTL-1; Arthritis; humoral immunity; Mouse model

*Corresponding author. Department of Pediatrics, Children's Hospital of Pittsburgh of UPMC, Rangos 9121, 4401 Penn Avenue, Pittsburgh, PA 15224, USA. Tel.: +1 412 692 9459; fax: +1 412 692 5565.

Disclosures: RH is named as an author in a patent filed by the University of Pittsburgh on FSTL-1 as a target in inflammatory conditions.

1. Introduction

Lyme disease, caused by infection with the spirochete *Borrelia burgdorferi,* is a multisystem infectious disease and is the most commonly reported vector-borne infection in the United States, with more than 20,000 cases occurring annually in the United States [1]. CDC data reveal Lyme arthritis to be present in 30% of patients [1], and associated with significant morbidity and cost. The first report of Lyme disease presented it as an unusual clustering of cases similar to juvenile idiopathic arthritis (JIA) [2]. While subsequent studies distinguished Lyme arthritis from other forms of autoimmune arthritis, Lyme disease shares many clinical, histologic and immune manifestations with autoimmune arthritides in both clinical studies and experimental models [3]. The clinical findings of large joint monoarthritis accompanied by more swelling and stiffness than acute inflammation distinguish Lyme from septic arthritis caused by pyogenic bacterial etiologies. Meanwhile, the slower onset and chronicity are shared with autoimmune disease. Histologic findings in Lyme and autoimmune arthritides can be identical. At a pathologic level, synovial infiltration and proliferation in Lyme arthritis is mediated by many of the same cytokines (e.g. TNF-α, IL-1β and IL-6) identified in models of JIA, such as collagen-induced arthritis (CIA) [4,5].

Follistatin-like protein 1 (FSTL-1), a TGF-β inducible gene, has recently been identified as a critical mediator in the development of CIA. FSTL-1 is highly conserved across mammalian species, with human and mouse FSTL-1 sharing 92% identity in their amino acid sequences. FSTL-1 gene transcription is upregulated in the synovium and synovial fluid of patients with JIA and rheumatoid arthritis [6,7]. Experimental in vivo models show FSTL-1 over-expression to exacerbate arthritis, and FSTL-1 blockade through exogenous antibody ameliorates arthritis in CIA in the DBA/1 murine strain [8]. In vitro and in vivo studies show that FSTL-1 activity is mediated by TNF-alpha, IL-1β, IL-6 and MCP-1 [9]. Study of the immune response of Lyme arthritis has identified similar cytokines (TNF-alpha, IL-1β and IL-6) as critical in the pathogenesis of Lyme arthritis during its development in human and murine models [10]. Given the critical role for FSTL-1 in CIA as well as the similarities between Lyme arthritis and RA, we hypothesized that FSTL-1 would mediate the inflammatory arthritis observed after *B. burgdorferi* infection.

We have previously shown that the DBA/1 mouse, the primary murine strain for the study of collagen-induced arthritis (CIA), serves as a model for the study of Lyme arthritis [11]. In the current study, we examined the role of FSTL-1 in the DBA/1 model of murine Lyme arthritis. We show that FSTL-1 is increased in response to *B. burgdorferi* infection in murine Lyme arthritis and that reduced FSTL-1 expression results in an attenuated arthritis phenotype and alterations in antigen recognition. These data show a critical role for FSTL-1 in mediating Lyme arthritis and antibody production.

2. Materials and methods

2.1. Animals

A 2565 bp insert containing *loxP* sequence was inserted within the *fstl-1* exon 1 along with a *flP* sequence, a *neomycin* cassette, a second *flP* site and second *loxP* site past exon 2 as a

germline mutation on a C57Bl/6 mouse background (H2 haplotype b). C57Bl/6 FSTL-1 homozygotes (fstl-$1^{fl/fl}$) were crossed to DBA/1 (Harlan Laboratories, Indianapolis, IN) Wild-type mice (H2 haplotype q) to generate double heterozygous mice (fstl-$1^{fl/wt}$ $H2^{b/q}$). Heterozygotes were then backcrossed onto the DBA/1 background and confirmed to be fstl-$1^{fl/fl}$ $H2^{q/q}$ by PCR screen and FACS analysis. Confirmed to have a 60% reduction in serum FSTL-1 and decreased tissue FSTL-1 mRNA production, these mice were considered hypomorphic for FSTL-1 (Fig. 2C). All experiments were performed in these FSTL-1 hypomorphic and WT DBA/1 mice at 6–8 weeks of age. Mice were housed and all experiments performed in accordance with the University of Pittsburgh School of Medicine Institutional Animal Care and Use Committee guidelines. All mouse experiments were performed under protocol #0807800A-3, which was approved by the Institutional Animal Care and Use Committee.

2.2. Identification of fstl-1 mouse alleles by PCR

Genomic DNA isolated from tail clippings taken from 21-day-old mice was used in 13 μL reactions containing Taq DNA Polymerase (Invitrogen). Each reaction contained FSTL-1 primers (forward ACTTCCTCGGAGCCTGGTGATAAG and reverse CGCTCAGACCCTAGAAACTTCTTCG) at 0.5 μM concentration. Cycle parameters were as follows: 1 cycle at 94 °C for 3 min, then 35 cycles of 94 °C for 45 s, 55 °C for 45 s, and 72 °C for 1 min 15 s, followed by 1 cycle at 72 °C for 10 min. FSTL-1 hypomorphic mice yielded a 238 bp band while wild-type mice yielded a 199 bp band (Fig. 2B).

2.3. B. burgdorferi culture and infection

Low-passage non-clonal B31 strain *B. burgdorferi* were cultured in BSK-H media (Sigma) at 35 °C and 5% CO_2. Bacteria were shifted to pH 7.0 BSK-H and grown to mid-log phase ($\sim 5 \times 10^7$ spirochetes/mL) as enumerated by dark-field microscopy. Groups of 10 mice were infected with 1×10^6 spirochetes subcutaneously in the mid back with sham-infected being injected with BSK-H media alone. Tibiotarsal joints were measured in duplicate by a blinded observer prior to infection and at least twice weekly in the anterio-posterior dimension with digital micrometers. Mice were sacrificed at 14 days post-infection (for examination of early disease, such as carditis) or 42 days post infection (for examination of arthritis) by carbon dioxide inhalation.

2.4. Histologic analysis of tibiotarsal joints

Upon sacrifice, one ankle from each mouse was placed in 10% neutral buffered formalin (Fisher Scientific, Pittsburgh, PA) until processing. Joints were decalcified and paraffin embedded, sectioned and stained with hematoxylin–eosin. Joints were blindly scored as follows on a scale of 0–3 by an independent pathologist; 0 – normal, no inflammation or synovial proliferation, 1 – focal mild synovial proliferation and/or inflammation, 2 – marked inflammation and/or synovial proliferation, affecting portion of the specimen and 3 – marked inflammation and synovial proliferation involving most or all of the specimen.

2.5. DNA extraction from infected tissues

Control and infected mice were sacrificed at 14 and 42 days post-infection, and one rear ankle joint and one half heart were stored immediately in dry ice and transferred to −80 °C until the time of DNA extraction. Each tissue was pulverized with liquid nitrogen pre-chilled mortar and pestle and transferred to 2.5 mL of a 1 mg/mL collagenase A (Boehringer Mannheim) solution in phosphate-buffered saline (pH 7.4). Digestions were carried out for 4 h at 37 °C. An equal volume of proteinase K solution (0.2 mg of proteinase K per mL, 200 mM NaCl, 20 mM Tris–HCl [pH 8.0], 50 mM EDTA, 1% sodium dodecyl sulfate) was added to collagenase digested tissues, and the mixture was incubated overnight at 55 °C. DNA was recovered by extraction of the digested sample with phenol-chloroform and subsequent ethanol precipitation. Resuspended samples were incubated with 0.1 mg/mL of DNase-free RNase for 1 h at 37 °C. Extractions and precipitations were repeated, and DNA was resuspended in 0.5 mL of TE. DNA concentration was determined by A260 and samples were used for quantitative PCR assays.

2.6. Measurement of spirochetal density by real-time qPCR

One hundred nanograms of extracted tissue DNA was used in 25 μL reactions containing SYBR® Green JumpStart™ Taq Ready-Mix™ (Sigma) using the iCycler iQ Detection System (Bio-Rad, Hercules, CA). Each reaction contained either OspC primers or mouse β-actin primers (Table 1) at 1 μM concentration. Cycle parameters were as follows: 1 cycle at 95 °C for 3 min, then 50 cycles of 95 °C for 15 s followed by 55 °C for 30 s. Melting curves were generated by 80 cycles of 50 °C for 10 s with 0.5 °C increments. qPCR reactions were performed in triplicate at least two times with comparable results. The results were calculated using the $\Delta\Delta C_t$ method, where relative amounts of *B. burgdorferi* DNA were compared to murine β-actin gene as an internal standard.

2.7. RNA extraction from infected tissues

Total RNA from homogenized heart and tibiotarsal joints was isolated using Trizol Reagent (Life Techonologies, Grand Island, NY) following the manufacturer's instructions. Briefly, 1 mL of Trizol Reagent was added to homogenized tissue and incubated at room temperature for 5 min. Chloroform (0.2 mL) was added to tissues, vortexed and incubated at room temperature for 3 min. Tubes were centrifuged at 12,000 × *g* for 15 min at 4 °C. Aqueous layer was added to 0.5 mL isopropyl alcohol, incubated at room temperature for 10 min and centrifuged again. The supernatant was removed, the pellet was washed with 75% EtOH and centrifuged at 7500 × *g* for 5 min at 4 °C. The supernatant was again removed, the pellet was air dried and resuspended in 50 μL nuclease-free water. Contaminating DNA was removed using RQ1 RNase-free DNase (Promega, Madison, WI). RNA was quantitated by absorbance at 260 nm and stored at −80 °C.

2.8. Quantitative RT-PCR analysis

qRT-PCR was performed using iScript One-Step RT-PCR with SYBR Green (Bio-Rad). Twenty-five microliter reactions were performed in duplicate in a 96-well format and reactions contained 264 nM concentrations of each primer (Table 1) and Reaction Mix diluted to 1×. RNA was then added to a final amount of 10 ng qRT-PCR conditions were as

follows: 1 cycle at 50 °C for 10 min, 1 cycle at 95 °C for 5 min, and 40 cycles of 95 °C for 10 s and 55 °C for 30 s. Melting curves were generated by 80 cycles of 50 °C for 10 s with 0.5 °C increments. The results were calculated using the comparative C_T method ($2^{-\Delta\Delta C_T}$) [12], where relative amounts of RNA were normalized to the housekeeping gene, *β-actin.* Changes in fluorescence were monitored by using the iCycler iQ Detection System (Bio-Rad, Hercules, CA). qRT-PCR reactions were performed in triplicate at least two times with comparable results.

2.9. Anti-B. burgdorferi ELISA

Costar high binding flat-bottom 96-well EIA/RIA plates (Corning) were coated with 200 ng of *B. burgdorferi* cell lysate in 0.1 M $NaHCO_3$, pH 8.6, covered and incubated overnight at 4 °C. Wells were washed twice with dH_2O and blocked with 5% milk in TBS-T_{20} (TBS with 0.02% Tween-20) (blocking buffer) for 1 h at 37 °C. Blocking buffer was removed and wells were incubated for 1 h at 37 °C with infected mouse serum (1:100 dilution) in blocking buffer. After washing with TBS-T_{20} (wash buffer), wells were incubated for 1 h at 37 °C with indicated secondary goat anti-mouse alkaline phosphatase conjugated antibody, IgM (μ-chain), IgG (whole molecule), IgG (γ-chain specific) (Sigma), IgG1, IgG2b or IgG3 (Southern Biotech). All Sigma antibodies were used at a 1:10,000 dilution and Southern Biotech antibodies were used at a 1:3000 dilution. Wells were washed and incubated with PNPP (Thermo Scientific) for 30 min at room temperature. After incubation with PNPP, the reaction was stopped with 2 N NaOH and absorbance at 405 nm was determined. Wells were read in duplicate.

2.10. FSTL-1 ELISA

FSTL-1 was assayed essentially as previously described [6] by coating Nunc Immunomodule MaxiSorp ELISA plates (Nalgene) with 100 μL of 2 μg/mL monoclonal rat anti-FSTL-1 (R&D Systems) overnight at 4 °C. Plates were washed with PBS/0.05% Tween-20 and blocked with 1% BSA/5% sucrose/0.05% Tween-20 for 1 h. Samples were incubated for 1 h at room temperature. Then, 2.5 μg/mL biotin-labeled polyclonal rabbit anti-FSTL-1 was added for 4 h. Plates were washed and incubated with streptavidin-HRP (Invitrogen), developed with a Peroxidase Substrate System ABTS (Kirkegaard & Perry Laboratories), and absorbance read at 405 nm on a microplate reader.

2.11. One-dimensional electrophoresis and immunoblotting

For one-dimensional electrophoresis, 15 μg of membrane proteins (prepared as previously described from fractionation of *B. burgdorferi* B31 strain) [13] were separated on sodium dodecyl sulfate polyacrylamide gels (SDS−PAGE) with an SE600 gel apparatus (Hoefer Scientific, San Francisco, CA). Gels were transferred to nitrocellulose (Bio-Rad Laboratories) as described by Towbin et al. with a Bio-Rad Trans Blot Cell (60 V for 2.5 h at 4 °C) [14]. After transfer, proteins were visualized by amido blue (0.1% amido blue dye in 1.0% acetic acid), and standards were marked. Membranes were blocked with blocking buffer (overnight at 4 °C) and probed with 1:1000 infected mouse serum in blocking buffer for 1 h at 25 °C. After washing, membranes were probed with 1:5000 HRP-conjugated goat anti-mouse IgG + IgM (Sigma) for 1 h at 25 °C. Membrane bands were visualized with the

ECL Western Blotting Detection Reagents (Amersham Biosciences) in accordance with the manufacturer's specifications.

2.12. Two-dimensional electrophoresis

Prior to two-dimensional electrophoresis, *B. burgdorferi* membrane proteins were precipitated using TCA-acetone as previously described [13]. Precipitated protein samples were solubilized for isoelectric focusing using IPG buffer (7 M urea, 2 M thiourea, 4.0% (wt/vol) CHAPS, 1.0% (vol/vol) Triton X-100, 100 mM DTT, and 0.5% IPGphor buffer pH 3−10 (GE Healthsciences)). Samples were clarified by ultracentrifugation (435,700 × *g* for 30 min at 23 °C). 50 μg of this clarified *B. burgdorferi* membrane protein was loaded onto 13 cm, pH 3–10 IPG strips (GE Healthsciences) and focused for 82,000 V h using the IPGphor III system (GE Healthsciences) (running conditions: 500 V for 1 h, 1500 V for 1 h, and 8000 V for 80,000 V h). IPG strips were stored at −80 °C until separated by mass using SDS−PAGE as described above. Prior to SDS−PAGE, IPG strips were equilibrated twice in 10 mL of SDS equilibration buffer (3 M urea, 2.0% SDS, 1% DTT, and 10% (vol/vol) glycerol in 125 mM Tris (pH 8.8)) for 10 min at 23 °C. Standard SDS−PAGE was performed with broad-range protein standards (Promega). SDS−PAGE gels were transferred to nitrocellulose membranes and Western blotting performed as described for one-dimensional electrophoresis.

2.13. Statistical analysis

All statistics were performed using Graph Pad Prism 5 (Graph-Pad, La Jolla, CA). Parametric data were analyzed using unpaired students *t*-test with or without Welch's correction as well as Mann−Whitney *U* test for non-parametric data. Data are reported as mean ± standard error of the mean.

3. Results

3.1. FSTL-1 hypomorphic mice develop attenuated arthritis following B. burgdorferi infection

We have previously described that the DBA/1 mouse is useful for the in vivo modeling of experimental Lyme arthritis, developing tibiotarsal joint swelling and histologic disease comparable to existing models, such as the C3H congenic strains. In order to determine the contribution of FSTL-1 to the development of arthritis after *B. burgdorferi* infection, we generated a DBA/1 strain with reduced expression of FSTL-1. Previous work has shown that homozygous *fstl1*−/− deletion is perinatal lethal [15,16]. We therefore generated FSTL-1 hypomorphic mice by inserting a 2565 bp gene sequence within exon 1 of the *fstl-1* gene (Fig. 1A). DBA/1 mice homozygous for this mutation were found to have decreased serum FSTL-1 production at baseline (Fig. 1C) and decreased joint *fstl1* expression 42 days after *B. burgdorferi* infection (Fig. 1D). We used these FSTL-1 hypomorphic mice in subsequent experiments to determine the effect of reduced FSTL-1 expression on experimental Lyme disease.

We first compared the phenotype of disease in DBA/1 wild-type and FSTL-1 hypomorphic mice infected with 10^6 *B. burgdorferi* subcutaneously. All infected mice, regardless of

genotype, developed tibiotarsal joint swelling compared to uninfected controls. However, joint swelling (Fig. 2A) was significantly attenuated on days 35 and 42 in FSTL-1 hypomorphic strain when compared to wild-type mice infected with *B. burgdorferi*. In addition to the measurements of gross joint swelling, histologic scoring of arthritis at day 42 confirmed that decreased swelling correlated with reduced histologic severity of arthritis (1.0 ± 0.3 vs. 0.2 ± 0.1, wild type versus FSTL-1 hypomorphic strain) (Fig. 2B). Tibiotarsal joints from wild-type mice demonstrated greater degrees of inflammatory infiltrate with occasional fibrosis of the joint on histopathologic examination (Fig. 2C, D), whereas FSTL-1 hypomorphic strain mice had almost normal joint histology (Fig. 2E, F). Decreased serum and tissue FSTL-1 expression therefore led to attenuated arthritis following *B. burgdorferi* infection.

3.2. FSTL-1 hypomorphic mice have attenuated B. burgdorferi tissue burden during later stages of infection

After noting reduced arthritis with decreased expression of *fstl-1*, we sought to characterize the infectious burden in affected tissues. Fig. 3 shows *B. burgdorferi* burden in heart and tibiotarsal joint tissues at day 14 and 42 post infection assessed by quantitative PCR for *ospC.* Wild type and FSTL-1 hypomorphic mice had similar infectious burden in joint tissue 14 days post infection (1083 ± 102 versus 395 ± 312 copies ospC/10^6 murine actin, p = 0.15). Spirochetal loads in cardiac tissue were also similar (13 ± 5.0 versus 22 ± 9.6 copies *ospC*/10^6 murine actin, p = 0.30). However, infectious burden 42 days post infection revealed significantly lower loads of *B. burgdorferi* in FSTL-1 hypomorphic mice in both joint (1717 ± 440 versus 8929 ± 2266 copies *ospC*/10^6 murine actin, p = 0.0015) and heart (75 ± 14.8 versus 6294 ± 2308 copies *ospC*/10^6 murine actin, p < 0.0001). These data suggest that early spirochete dissemination is similar between wild type and FSTL-1 hypomorphic mice, but that tissue infection is more efficiently cleared in the FSTL-1 hypomorphic strain, possibly attenuating arthritis development. This difference in arthritis phenotype is not due to decreased infection of target tissues during initial infection, but occurs after target tissue infection has been established and the host immune response attempts to clear the spirochete.

3.3. FSTL-1 influences inflammatory cytokine production in vivo

The development of arthritis in the murine model of Lyme disease is characterized by the increase in expression of specific proinflammatory cytokines such as TNF-α, IL-1β and IL-6. We examined the expression of these cytokines in target tissues to determine how decreased infectious burden and histopathology correlated with expression of proinflammatory cytokines.

Cardiac expression between wild type and FSTL-1 hypomorphic mice 14 days post infection (Fig. 4A) of IL-6 (5.84 ± 0.63 versus 8.10 ± 3.67 copies *il-6*/10^6 murine actin, p = 0.84), IL-1β (99.5 ± 15.12 versus 99.48 ± 26.86 copies *il-1β*/10^6 murine actin, p = 0.60) and TNF-α (11.52 ± 1.90 versus 10.46 ± 2.75 copies *tnfα*/10^6 murine actin, p = 1.00) was not significantly different. However, 42 days post infection IL-6 was significantly elevated (16.34 ± 3.70 versus 7.15 ± 1.51 copies *il-6*/10^6 murine actin, p = 0.035), and IL-1β trended toward significance (152.7 ± 23.05 versus 97.10 ± 12.72 copies *il-1β*/10^6 murine actin, p =

0.09), in wild-type heart tissue when compared to FSTL-1 hypomorphic mice, despite an absence of histopathologic differences (data not shown). Cardiac TNF-α expression was not significantly different 42 days post infection (12.08 ± 2.85 versus 6.71 ± 1.52 copies *tnfa*/10^6 murine actin, $p = 0.84$).

Fig. 4B shows tibiotarsal joint expression of these same cytokines at day 14 and 42 post infection in wild type and FSTL-1 hypomorphic mice. We noted FSTL-1 hypomorphic mice to have a trend toward significantly reduced expression of TNF-α (11.74 ± 1.33 versus 7.10 ± 1.19 copies *tnfa*/10^6 murine actin, $p = 0.15$) and IL-6 (10.8 ± 1.00 versus 7.84 ± 1.19 copies *il-6*/10^6 murine actin, $p = 0.12$) in joints 14 days post infection, but similar IL-1β (125.2 ± 10.43 versus 129.2 ± 30.46 copies *il-1β*/10^6 murine actin, $p = 0.60$) expression. Interestingly, at 42 days post infection, corresponding with the peak of joint swelling and histopathologic arthritis severity, IL-1β (233.7 ± 21.18 versus 177.7 ± 44.41 copies *il-1β*/10^6 murine actin, $p = 0.019$) was significantly decreased in FSTL-1 hypomorphic joint tissue compared to wild type. TNF-α (8.47 ± 1.62 versus 7.57 ± 1.11 copies *tnfa*/10^6 murine actin, $p = 0.88$) and IL-6 (16.4 ± 6.43 versus 18.48 ± 7.85 copies *il-6*/10^6 murine actin, $p = 0.97$) expression were not different between the two groups. These data suggest that upon *B. burgdorferi* infection, reduction in FSTL-1 led to reduced joint swelling and arthritis which was associated with reduced inflammatory cytokine production.

3.4. FSTL-1 influences immunoglobulin production in response to B. burgdorferi infection

Previous work has established a critical role for humoral immunity in the clearance of *B. burgdorferi* infection [17]. Studies of Lyme arthritis in murine models of immune dysfunction show that B cell deficient mice demonstrate impairment of clearance and exaggerated inflammation when compared to T cell deficient mice [18]. Given its importance to immunity against *B. burgdorferi*, we sought to characterize the humoral response in FSTL-1 hypomorphic mice compared to wild type to determine if enhanced humoral responses might underlie the improved clearance of *B. burgdorferi* infection in this model. Fig. 5 shows ELISA data obtained using class- and isotype-specific secondary antibodies to detect averages of individual murine sera reactivity with *B. burgdorferi* membrane proteins. Sera were used from animals 14 and 42 days post infection.

FSTL-1 hypomorphic mice showed a trend toward reduced antibody production against *Borrelia* antigen at day 14, although none of the analyzed antibodies were significantly different. Comparison between DBA/1 wild-type and FSTL-1 hypomorphic mice indicated that total IgG/IgM (OD 0.188 ± 0.047 versus 0.122 ± 0.014, $p = 0.29$), IgM (OD 0.178 ± 0.007 versus 0.156 ± 0.023, $p = 0.34$), and IgG (OD 0.152 ± 0.050 versus 0.074 ± 0.013, $p = 0.22$) showed a nonsignificant trend toward higher levels in wild-type mice. Examination of IgG subclasses comparing wild-type and FSTL-1 hypomorphic mice at 14 days post infection showed this trend to be reflected in IgG2a (OD 0.114 ± 0.034 versus 0.050 ± 0.014, $p = 0.11$) and IgG3 (OD 0.084 ± 0.018 versus 0.422 ± 0.018, $p = 0.29$).

However, these antibody production trends were not sustained upon evaluation of serum 42 days post infection. DBA/1 wild-type and FSTL-1 hypomorphic mice had similar total IgG/IgM (OD 0.364 ± 0.022 versus 0.368 ± 0.026, $p = 0.94$) and IgG (OD 0.339 ± 0.013 versus 0.372 ± 0.024, $p = 0.34$). Comparing wild-type and FSTL-1 hypomorph IgM (OD

0.076 ± 0.005 versus 0.066 ± 0.006, $p = 0.38$) production showed it to be equally decreased by 42 days post infection. IgG subclass comparison between wild-type and FSTL-1 hypomorphic mice at 42 days post infection showed similar IgG2a production (OD 0.221 ± 0.016 versus 0.224 ± 0.027, $p = 0.76$) but a trend toward significantly decreased IgG3 (OD 0.246 ± 0.037 versus 0.175 ± 0.036, $p = 0.15$) in FSTL-1 hypomorphic mice. IgG1 was nearly undetectable in wild type and FSTL-1 hypomorphic mice at 14 days (OD 0.016 ± 0.005 versus 0.014 ± 0.007) and 42 days post infection (OD 0.040 ± 0.006 versus 0.009 ± 0.003).

3.5. FSTL-1 influences specific antigen recognition by humoral responses in DBA/1 mice infected by B. burgdorferi

The trends toward decreased anti-*Borrelia* immunoglobulin production led us to further examine antigen specificity in the serum antibody pool to determine if FSTL-1 had an influence on specific antigen recognition. Fig. 6A shows one-dimensional Western blots of *B. burgdorferi* membrane proteins probed with pooled wild type and FSTL-1 hypomorphic mouse sera 42 days post infection. We noted similar antigen recognition but a decrease in antibody reactivity in FSTL-1 hypomorphic mice which was consistent with our ELISA data. In order to identify individual antigens targeted by these sera, we performed two-dimensional electrophoresis using immobilized pH gradients (IPG) for first dimension separation by isoelectric point, and SDS-PAGE for second dimension separation by mass. Western blots of two-dimensional *B. burgdorferi* membrane protein separation show the immunoreactivity of pooled wild-type and FSTL-1 hypomorphic mouse sera separated by pI and mass (Fig. 6B). We were able to identify specific antigen targets using our previous work on the *Borrelia* proteome in addition to confirmation of key spots by proteomic analysis (data not shown) [11,13]. DBA/1 wild-type sera identified a greater number of antigens when compared to FSTL-1 hypomorphic mice. Certain antigens, such as OppA and RevA, were poorly detected by FSTL-1 hypomorphic serum. A majority of antigens (including ErpA, OspC, BmpA and other commonly recognized *Borrelia* membrane proteins) showed similar antibody density in the hypomorphic strains. These data show FSTL-1 hypomorphic mice have antigen-specific alterations in humoral response at 42 days post infection. It is notable that this difference in humoral response is in the setting of similar infectious burden at 14 days post infection despite decreased inflammation and improved spirochetal clearance. This data suggests that differences in antigen recognition are not solely due to a decrease in spirochetal load earlier in infection.

4. Discussion

Since its first description, Lyme disease, an infectious arthritis caused by *B. burgdorferi*, has been recognized as sharing clinical findings with autoimmune arthritides. Extensive investigation has revealed that the clinical and experimental data in these disorders share many similarities, including phenotypic, histologic and immunologic findings. Both diseases often present clinically as mono- or oligo-arthritis. Histopathologic correlates of joint involvement have shown leukocytic infiltration and synovial proliferation, with a relative absence of the destructive synovial pathology typical of septic arthritis caused by pyogenic organisms such as *Staphylococcus aureus*. Increasing understanding of the importance of

cellular and humoral involvement in these diseases has led to a central role for proinflammatory cytokines, including TNF-α, IL-1β and IL-6 [4,5]. Disruption of the proinflammatory cytokine signaling pathways and cellular involvement has been critical to investigations into the treatment of these parallel conditions.

Having recently described follistatin-like protein 1 (FSTL-1) as a proinflammatory molecule involved in the development of joint inflammation in rheumatoid arthritis [6], juvenile idiopathic arthritis [7] and the experimental model collagen induced arthritis [8] we sought to evaluate the involvement of FSTL-1 in experimental Lyme arthritis. Studies characterizing the involvement of FSTL-1 in CIA have been performed in the DBA/1 mouse strain, a standard murine strain for CIA [6,8]. We have recently demonstrated that the DBA/1 strain is a model for the study of Lyme arthritis, as the DBA/1 mouse develops joint swelling and histopathology similar to the C3H congenic strains which have been the primary murine model for the study of Lyme arthritis. Further, we found that infectivity and spirochete burden in target tissues such as joint and heart were comparable between the two strains [11]. Based on these data and the previous work by our group on FSTL-1, we hypothesized that FSTL-1 would be involved in murine Lyme arthritis, and that reduction of its expression would lead to attenuated disease.

The data presented here confirm that *B. burgdorferi* infection increases FSTL-1 production in vitro and in vivo, and that global reduction of FSTL-1 expression in our hypomorphic murine strain was associated with attenuation of joint swelling and reduction of the histopathologic severity of arthritis. We determined that tissue burden of spirochetes was similar in the first two weeks after infection, suggesting that early dissemination of bacteria was not significantly altered by the reduced FSTL-1 expression. However, at time points later in infection during the point of maximal joint swelling, spirochetal burden was significantly reduced in FSTL-1 hypomorphic target tissues. These data, along with reduced proinflammatory cytokine production, provide a mechanism for the observed reduction in the severity of inflammation in these mice.

These observations are significant for several reasons. They represent the first report describing FSTL-1 and the response to infection, in our study the spirochete *B. burgdorferi*. This infection likely serves as an excellent model to explore the role of FSTL-1 in response to pathogens, as FSTL-1 has been shown to be highly expressed in neurologic [19,20], cardiac [21–23] and other connective tissues [24,25], mostly of the mesenchymal lineage; all tissues targeted during *B. burgdorferi* infection. Further, FSTL-1 expression and function has been correlated with important non-infectious processes including sensory neuron signaling [20] and cardiomyocyte function [26], suggesting that FSTL-1 functions in normal development and physiology as well as mediating pathology. We had previously reported FSTL-1 to be elevated in the serum of patients with acute Kawasaki Disease [23] and that in experimental models, cardiac expression of *fstl-1* was induced by LPS injection. Although *B. burgdorferi* does not produce LPS, much of its membrane structure and microbiologic characteristics are similar to Gram negative bacteria. Surprisingly in our study, reduction of FSTL-1 production was associated with reduction of disease, from arthritic swelling and histopathology to spirochetal burden. The majority of studies of reduced innate and acquired immune system function in *Borrelia* infection are associated with an increased burden of

infection. A typical example of this is the TLR-2 knockout mouse, which experiences increased tissue burden, decreased clearance of bacteria, and increased severity of arthritis. However, our current findings regarding FSTL-1 share similarities to studies describing the role of IL-10 in *Borrelia* infection [27]. Examining infectivity and arthritis production comparing the C3H murine strain and arthritis-resistant C57Bl/6 strain, the authors concluded that C57Bl/6 mice have relative innate immune suppression, decreased target tissue *B. burgdorferi* burden and an attenuated arthritis phenotype compared to WT C3H mice as a result of C57Bl/6 mice having higher inducible levels of IL-10. Interestingly, C57Bl/6 IL-$10^{-/-}$ mice had further decreased *B. burgdorferi* burden in target tissues, yet developed more severe arthritis than C57Bl/6 IL-$10^{WT/WT}$. These findings suggest that IL-10 signaling pathways are important in controlling inflammation, arthritis development and clearing infection following *B. burgdorferi* infection; studies examining the effects of FSTL-1 on IL-10 function are ongoing. Descriptions of other immune targets with dual antimicrobial and anti-inflammatory functions are emerging as novel strategies to treat infectious diseases [28,29].

Humoral immunity is a key for the development and control of Lyme arthritis in natural infection, but is inadequate to completely clear spirochetes in T-cell deficient mice [17,30]. B cell responses however develop in the absence of T cell or innate immune components (TLR2 and MyD88), and passive antibody transfer or immunization of TLR2 $^{-/-}$ mice can be partially or completely protective [31]. We also assayed the humoral response in wild-type and FSTL-1 hypomorphic mice, hypothesizing that the improved clearance of bacteria from the tissues might be promoted by a superior antibody response in the hypomorphic strain. Interestingly, we observed impairment of the humoral response, though not clearly related to immunoglobulin class or isotype, but rather with limited antigen recognition as assessed by 2-dimensional Western blotting. Whether these findings represent an FSTL-1 host effect on *Borrelia* gene expression, or correspond with FSTL-1 dependent antigen presentation is being actively studied.

Our study has limitations. The infectious dose employed (10^6 spirochetes/animal) is above the threshold required for infectivity, though we have previously shown this dose to successfully produce arthritis in the DBA/1 strain [11], as have others in different strains [32]. Our data does not address the possibility that lower spirochetal doses might produce an alternate effect on FSTL-1 in DBA/1 wild-type or hypomorphic mice. We also evaluated humoral responses by Western blot using pooled sera, which may mask the individual variability of serologic response to specific antigens. We did however observe that on individual one-dimensional immunoblots, the frequency of individual reactivity correlated well with antigen recognition of pooled sera (data not shown). The absence of a full knockout of the *fstl-1* gene in DBA/1 is another limitation – our FSTL-1 hypomorphic strain still produced a detectable level FSTL-1, albeit significantly reduced compared to wild-type mice. The perinatal lethal effect of homozygous *fstl-1* deletion previously reported led us to this strategy, but future studies examining the role of FSTL-1 in conditional knockouts are of great interest to our laboratory. Finally, although we detected differences in cardiac infection and cytokine expression in our study, experimental Lyme carditis in the mouse currently lacks a measurable phenotypic correlate of infection in live animals similar to joint

measurements for arthritis, thus differences in the cardiac manifestations of experimental Lyme disease may have gone undetected.

The identification of FSTL-1 as a critical mediator of the pathogenesis and immune response of murine Lyme arthritis is an important step in our understanding the role of FSTL-1 in the host response to infection. While our study only addresses the experimental Lyme arthritis model, it suggests that investigation of the role of FSTL-1 in other infectious processes may be valuable. Further study of the role of this molecule in Lyme arthritis may provide insight into the development of inflammation which leads to the phenotype of Lyme arthritis. Of important clinical benefit, FSTL-1 may be as a novel target for interruption of the inflammatory and pathologic events associated with Lyme disease.

Acknowledgments

This work was supported by National Institutes of Health grants R01 AR056959 (RH), T32 AR052282 (RH and BC), K08 AI072365 (AN), and the Children's Hospital of Pittsburgh Research Advisory Committee (AN).

References

1. Bacon RM, Kugeler KJ, Mead PS. Surveillance for Lyme disease–United States, 1992-2006. MMWR Surveill Summ. 2008; 57:1–9. [PubMed: 18830214]
2. Steere AC, Malawista SE, Snydman DR, Shope RE, Andiman WA, Ross MR, et al. Lyme arthritis: an epidemic of oligoarticular arthritis in children and adults in three connecticut communities. Arthritis Rheum. 1977; 20:7–17. [PubMed: 836338]
3. Harjacek M, Diaz-Cano S, Alman BA, Coburn J, Ruthazer R, Wolfe H, et al. Prominent expression of mRNA for proinflammatory cytokines in synovium in patients with juvenile rheumatoid arthritis or chronic Lyme arthritis. J Rheumatol. 2000; 27:497–503. [PubMed: 10685820]
4. McInnes IB, Schett G. Cytokines in the pathogenesis of rheumatoid arthritis. Nat Rev Immunol. 2007; 7:429–42. [PubMed: 17525752]
5. Miller JC, Ma Y, Crandall H, Wang X, Weis JJ. Gene expression profiling provides insights into the pathways involved in inflammatory arthritis development: murine model of Lyme disease. Exp Mol Pathol. 2008; 85:20–7. [PubMed: 18462718]
6. Clutter SD, Wilson DC, Marinov AD, Hirsch R. Follistatin-like protein 1 promotes arthritis by up-regulating IFN-gamma. J Immunol. 2009; 182:234–9. [PubMed: 19109154]
7. Wilson DC, Marinov AD, Blair HC, Bushnell DS, Thompson SD, Chaly Y, et al. Follistatin-like protein 1 is a mesenchyme-derived inflammatory protein and may represent a biomarker for systemic-onset juvenile rheumatoid arthritis. Arthritis Rheum. 2010; 62:2510–6. [PubMed: 20506332]
8. Miyamae T, Marinov AD, Sowders D, Wilson DC, Devlin J, Boudreau R, et al. Follistatin-like protein-1 is a novel proinflammatory molecule. J Immunol. 2006; 177:4758–62. [PubMed: 16982916]
9. Chaly Y, Marinov AD, Oxburgh L, Bushnell DS, Hirsch R. FSTL1 promotes arthritis in mice by enhancing inflammatory cytokine/chemokine expression. Arthritis Rheum. 2012; 64:1082–8. [PubMed: 22006268]
10. Crandall H, Dunn DM, Ma Y, Wooten RM, Zachary JF, Weis JH, et al. Gene expression profiling reveals unique pathways associated with differential severity of lyme arthritis. J Immunol. 2006; 177:7930–42. [PubMed: 17114465]
11. Campfield BT, Nolder CL, Davis A, Hirsch R, Nowalk AJ. The DBA/1 strain is a novel mouse model for experimental Borrelia burgdorferi infection. Clin Vaccine Immunol. 2012; 19:1567–73. [PubMed: 22855391]
12. Livak KJ, Schmittgen TD. Analysis of relative gene expression data using realtime quantitative PCR and the 2(−Delta Delta C(T)) method. Methods. 2001; 25:402–8. [PubMed: 11846609]

13. Nowalk AJ, Gilmore RD Jr, Carroll JA. Serologic proteome analysis of Borrelia burgdorferi membrane-associated proteins. Infect Immun. 2006; 74:3864–73. [PubMed: 16790758]
14. Towbin H, Staehelin T, Gordon J. Electrophoretic transfer of proteins from polyacrylamide gels to nitrocellulose sheets: procedure and some applications. Proc Natl Acad Sci U S A. 1979; 76:4350–4. [PubMed: 388439]
15. Geng Y, Dong Y, Yu M, Zhang L, Yan X, Sun J, et al. Follistatin-like 1 (Fstl1) is a bone morphogenetic protein (BMP) 4 signaling antagonist in controlling mouse lung development. Proc Natl Acad Sci U S A. 2011; 108:7058–63. [PubMed: 21482757]
16. Sylva M, Li VS, Buffing AA, van Es JH, van den Born M, van der Velden S, et al. The BMP antagonist follistatin-like 1 is required for skeletal and lung organogenesis. PloS One. 2011; 6:e22616. [PubMed: 21826198]
17. Kraiczy P, Skerka C, Kirschfink M, Zipfel PF, Brade V. Immune evasion of *Borrelia burgdorferi*: insufficient killing of the pathogens by complement and antibody. Int J Med Microbiol. 2002; 291(Suppl. 33):141–6. [PubMed: 12141738]
18. Wooten RM, Weis JJ. Host-pathogen interactions promoting inflammatory Lyme arthritis: use of mouse models for dissection of disease processes. Curr Opin Microbiol. 2001; 4:274–9. [PubMed: 11378478]
19. Li KC, Wang F, Zhong YQ, Lu YJ, Wang Q, Zhang FX, et al. Reduction of follistatin-like 1 in primary afferent neurons contributes to neuropathic pain hypersensitivity. Cell Res. 2011; 21:697–9. [PubMed: 21423271]
20. Li KC, Zhang FX, Li CL, Wang F, Yu MY, Zhong YQ, et al. Follistatin-like 1 suppresses sensory afferent transmission by activating Na+,K+-ATPase. Neuron. 2011; 69:974–87. [PubMed: 21382556]
21. Ogura Y, Ouchi N, Ohashi K, Shibata R, Kataoka Y, Kambara T, et al. Therapeutic impact of follistatin-like 1 on myocardial ischemic injury in preclinical models. Circulation. 2012; 126:1728–38. [PubMed: 22929303]
22. Shimano M, Ouchi N, Nakamura K, van Wijk B, Ohashi K, Asaumi Y, et al. Cardiac myocyte follistatin-like 1 functions to attenuate hypertrophy following pressure overload. Proc Natl Acad Sci U S A. 2011; 108:E899–906. [PubMed: 21987816]
23. Gorelik M, Wilson DC, Cloonan YK, Shulman ST, Hirsch R. Plasma follistatin-like protein 1 is elevated in Kawasaki disease and may predict coronary artery aneurysm formation. J Pediatrics. 2012; 161:116–9.
24. Wang Y, Li D, Xu N, Tao W, Zhu R, Sun R, et al. Follistatin-like protein 1: a serum biochemical marker reflecting the severity of joint damage in patients with osteoarthritis. Arthritis Res Ther. 2011; 13:R193. [PubMed: 22117761]
25. Umezu T, Yamanouchi H, Iida Y, Miura M, Tomooka Y. Follistatin-like-1, a diffusible mesenchymal factor determines the fate of epithelium. Proc Natl Acad Sci U S A. 2010; 107:4601–6. [PubMed: 20176958]
26. Oshima Y, Ouchi N, Sato K, Izumiya Y, Pimentel DR, Walsh K. Follistatin-like 1 is an Akt-regulated cardioprotective factor that is secreted by the heart. Circulation. 2008; 117:3099–108. [PubMed: 18519848]
27. Brown JP, Zachary JF, Teuscher C, Weis JJ, Wooten RM. Dual role of interleukin-10 in murine Lyme disease: regulation of arthritis severity and host defense. Infect Immun. 1999; 67:5142–50. [PubMed: 10496888]
28. Capparelli R, Romanelli A, Iannaccone M, Nocerino N, Ripa R, Pensato S, et al. Synergistic antibacterial and anti-inflammatory activity of temporin A and modified temporin B in vivo. PloS One. 2009; 4:e7191. [PubMed: 19784377]
29. Som A, Navasa N, Percher A, Scott RW, Tew GN, Anguita J. Identification of synthetic host defense Peptide mimics that exert dual antimicrobial and anti-inflammatory activities. Clin Vaccine Immunol. 2012; 19:1784–91. [PubMed: 22956655]
30. Dickinson GS, Alugupalli KR. Deciphering the role of Toll-like receptors in humoral responses to Borreliae. Front Biosci Sch Ed. 2012; 4:699–712.

31. Wooten RM, Ma Y, Yoder RA, Brown JP, Weis JH, Zachary JF, et al. Toll-like receptor 2 is required for innate, but not acquired, host defense to Borrelia burgdorferi. J Immunol. 2002; 168:348–55. [PubMed: 11751980]

32. Schaible UE, Gern L, Wallich R, Kramer MD, Prester M, Simon MM. Distinct patterns of protective antibodies are generated against *Borrelia burgdorferi* in mice experimentally inoculated with high and low doses of antigen. Immunol Lett. 1993; 36:219–26. [PubMed: 8349316]

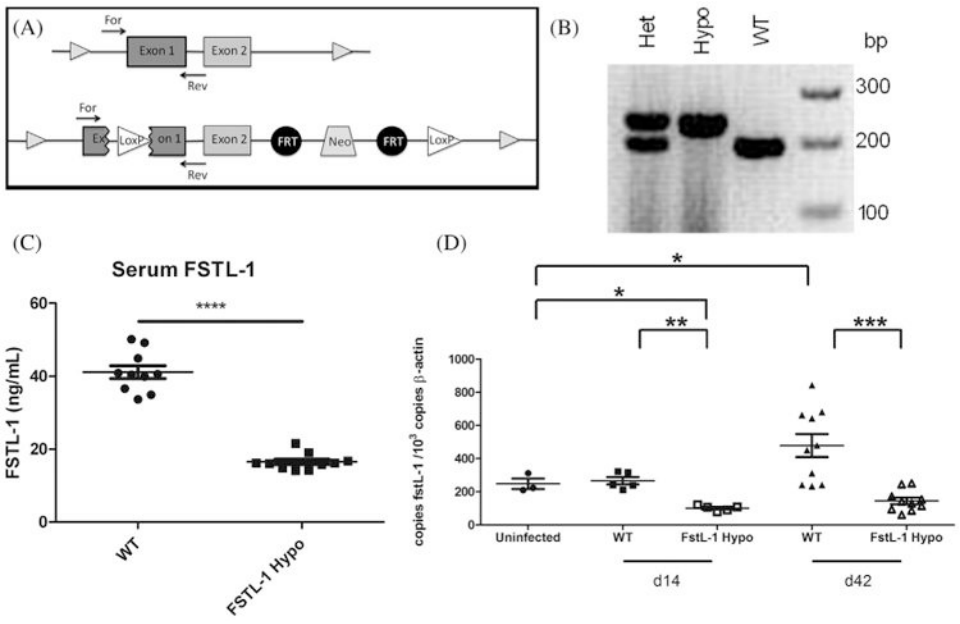

Fig. 1.

FSTL-1 hypomorphic mice have decreased *fstl-1* gene transcription and FSTL-1 serum protein. (A). A 2565 bp insert containing *loxP* sequence was inserted within the *fstl-1* exon 1 along with *flP*, a *neomycin* cassette, a second *flP* and second *loxP* site, and was (B) detectable by PCR as FSTL-1 hypomorphic mice yielded a 238 bp gene product (hypo) while wild-type (WT) mice yielded a 199 bp band; in heterozygotes (het) both gene products were detectable. (C) This insertion resulted in FSTL-1 hypomorphic mice with a 60% reduction in serum FSTL-1 (D). Hypomorphic mice showed a reduction in joint *fstl-1* transcription versus wild-type mice at day 14 and 42 post infection. Data are representative of at least two individual experiments with $n = 10$ mice/treatment group. $^{**}p < 0.01$, $^{***}p < 0.001$, $^{****}p < 0.0001$.

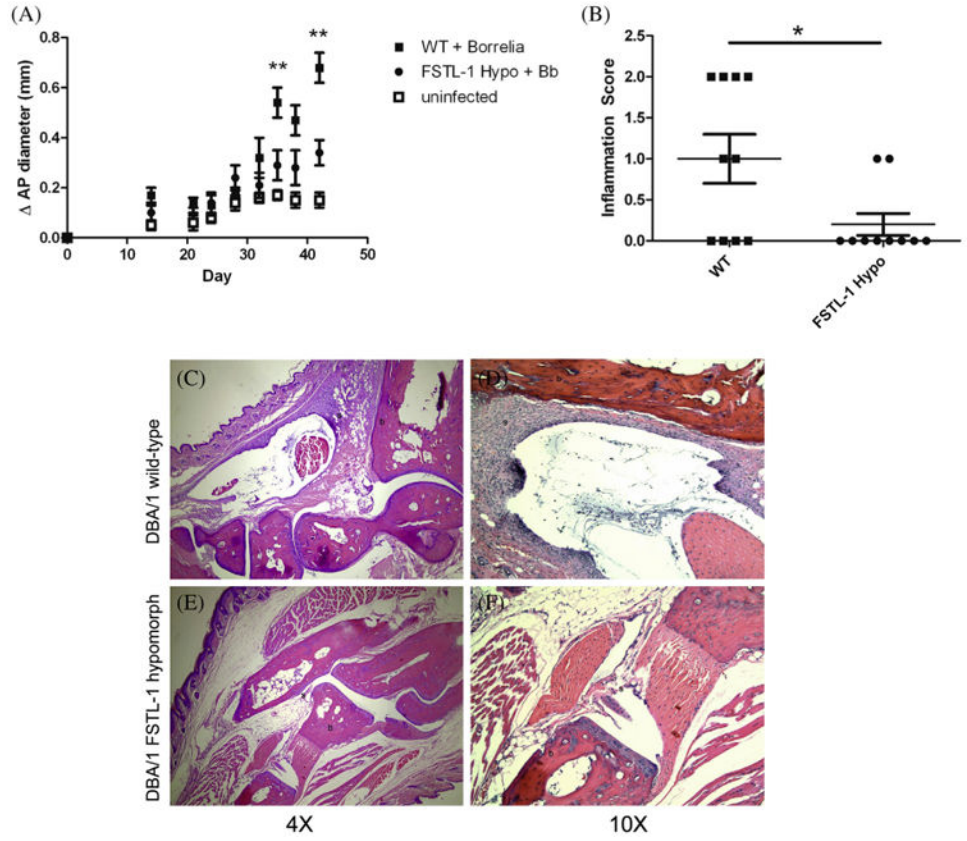

Fig. 2.

FSTL-1 mediates the development of Lyme arthritis. (A) DBA/1WT (squares) and FSTL-1 hypomorph mice (circles) were infected with 10^6 *Borrelia burgdorferi* (solid) or media alone (open). (B) H&E stained tibiotarsal joints of day 42 *Borrelia burgdorferi*-infected WT and FSTL-1 hypomorph mice were scored for inflammation. Shown are representative 4× (C, E) and 10× (D, F) images of day 42 *Bb* infected WT (C, D) and FSTL-1 hypomorphic (E, F) mice. Arrow denotes synovial proliferation. b, Bone; s, synovium. *$p = 0.03$; **$p < 0.01$. Data are representative of at least two individual experiments with $n = 10$ mice/treatment group.

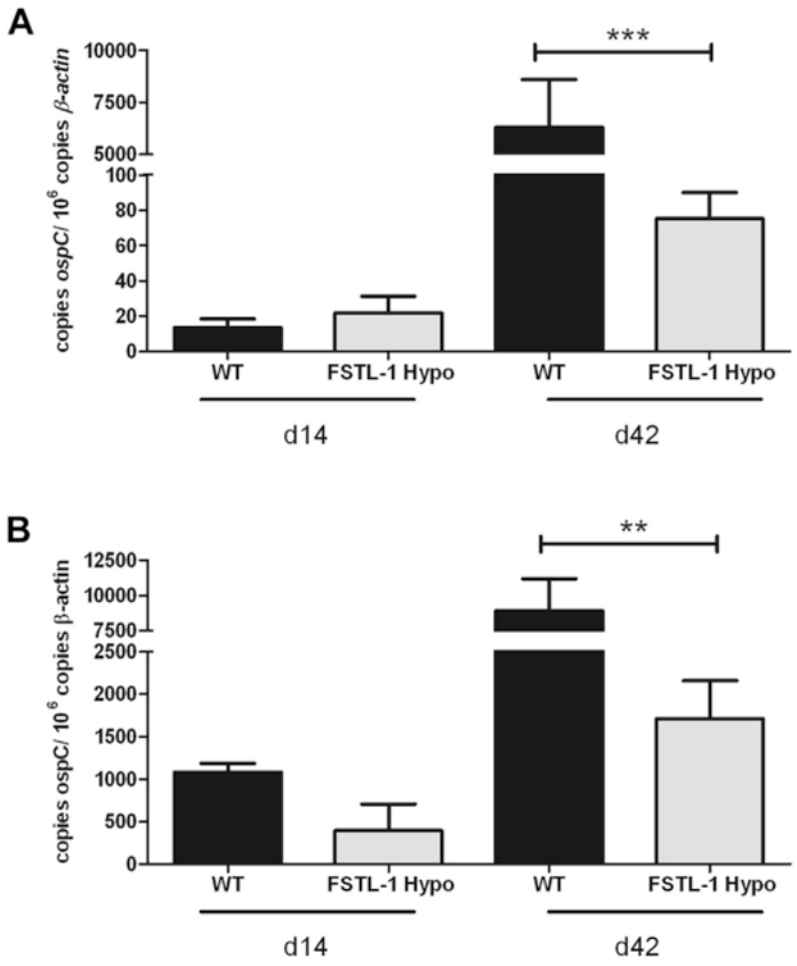

Fig. 3.

FSTL-1 hypomorphic mice have attenuated *Borrelia burgdorferi* burden in target tissues. qPCR for *ospC* of extracted DNA from (A) hearts and (B) joints of WT and FSTL-1 hypomorph mice 14 and 42 days post infection with 10^6 *Borrelia burgdorferi*. Error bars represent SEM. Data are representative of at least two individual experiments with $n = 10$ mice/treatment group. $^{**}p < 0.01$; $^{***}p < 0.001$.

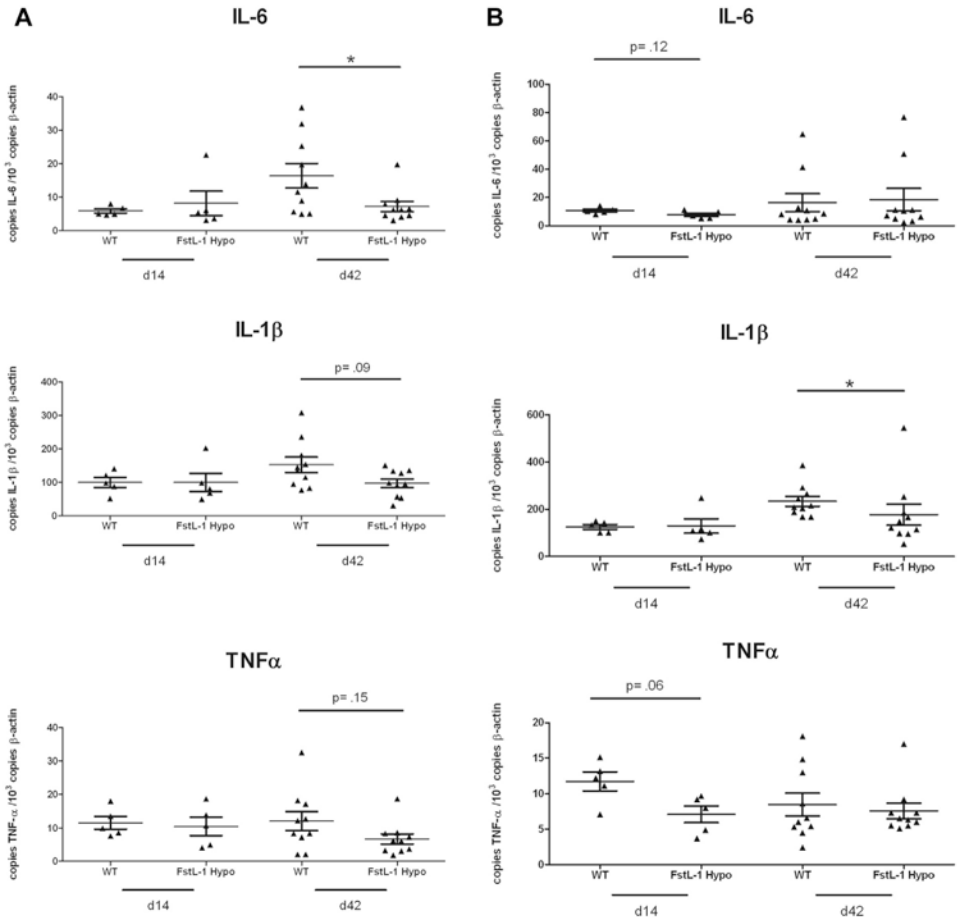

Fig. 4.

FSTL-1 influences inflammatory cytokine production in vivo. WT and FSTL-1 hypomorph mice were infected with 10^6 *Borrelia burgdorferi* and qRT-PCR performed on (A) hearts and (B) joints for IL-6, IL-1β and TNFα at indicated time points. $n = 10$ mice/treatment group. Each dot represents an individual animal tissue. Bars represent mean for each treatment group. $*p < 0.05$.

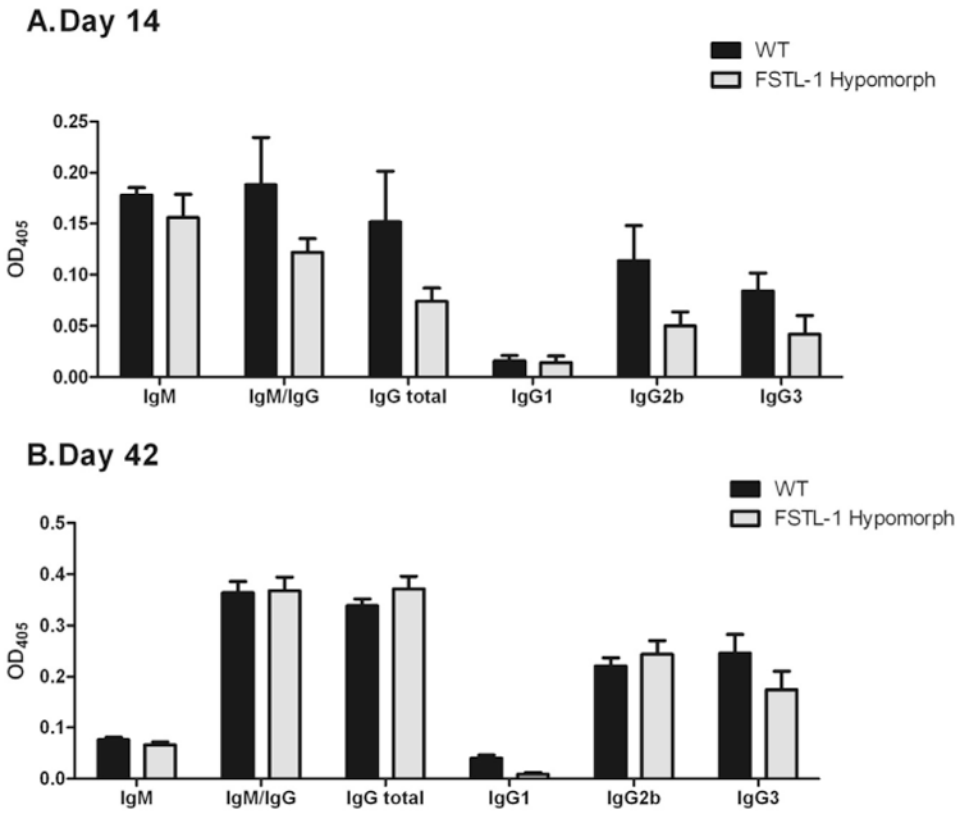

Fig. 5.

FSTL-1 influences immunoglobulin production in response to *B. burgdorferi* infection. ELISA plates coated with *B. burgdorferi* membrane-associated proteins were probed with individual *B. burgdorferi*-infected DBA/1 WT and FSTL-1 hypomorphic mouse serum and detected using class- and isotype-specific secondary antibodies at (A) 14 days post infection and (B) 42 days post infection. Data are representative of at least two individual experiments with $n = 10$ mice/treatment group. Each ELISA was performed ≥3 times. Mean values are depicted with standard error.

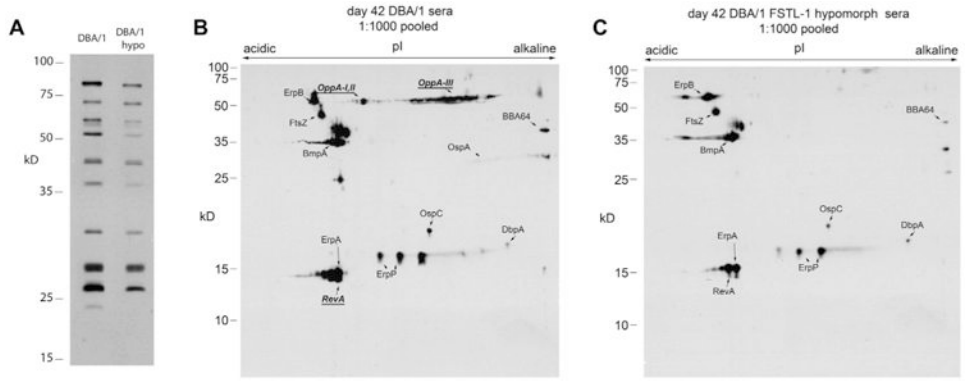

Fig. 6.

FSTL-1 is critical to *Borrelia burgdorferi* antigen recognition. (A) *B. burgdorferi* membrane-associated proteins (MAP) (15 μg) separated by one-dimensional SDS–PAGE were probed with pooled serum (n = 10 per group) from WT and FSTL-1 hypomorphic mice at 42 days post *B. burgdorferi* infection with detection of polyclonal IgG/IgM reactivity. Fifty micrograms of *B. burgdorferi* MAP were separated using IPG followed by SDS–PAGE and transferred to nitrocellulose membrane. Pooled sera from both (B) WT and (C) FSTL-1 hypomorphic mice (n = 10) were used to probe blots followed by detection of polyclonal IgG/IgM reactivity. Resulting two-dimensional serologic maps were correlated with previously identified proteins. Bold and underlined proteins indicate MAPs recognized by WT but not FSTL-1 hypomorphic serum. Data are representative of two individual experiments with n = 10 mice/treatment group.

Table 1

Primers used in qPCR and qRT-PCR.

β-actin	For	AGAGGGAAATCGTGCGTGAC
	Rev	CAATAGTGATGACCTGGCCGT
OspC	For	TACGGATTCTAATGCGGTTTTAC
	Rev	GTGATTATTTTCGGTATCCAAACCA
FstL-1	For	AACAGCCATCAACATCACCA
	Rev	GGCACTTGAGGAACTCTTGG
IL-6	For	GAGGATACCACTCCCAACAGACC
	Rev	AAGTGCATCATCGTTGTTCATACA
IL-1β	For	CAACCAACAAGTGATATTCTCCATG
	Rev	GATCCACACTCTCCAGCTGCA
TNF-α	For	CATCTTCTCAAAATTCGAGTGACAA
	Rev	TGGGAGTAGACAAGGTACAACCC